Evaluation of thieno[3,2-b]pyrrole[3,2-d]pyridazinones as activators of the tumor cell specific M2 isoform of pyruvate kinase

Jian-kang Jiang [a], Matthew B. Boxer [a], Matthew G. Vander Heiden [b,c,d], Min Shen [a], Amanda P. Skoumbourdis [a], Noel Southall [a], Henrike Veith [a], William Leister [a], Christopher P. Austin [a], Hee Won Park [e,f], James Inglese [a], Lewis C. Cantley [c,g], Douglas S. Auld [a], Craig J. Thomas [a,*]

[a] NIH Chemical Genomics Center, National Human Genome Research Institute, National Institutes of Health, 9800 Medical Center Drive, Rockville, MD 20850, USA
[b] Koch Institute at MIT, Cambridge, MA 02139, USA
[c] Dana Farber Cancer Institute, Boston, MA 02115, USA
[d] Department of Systems Biology, Harvard Medical School, Boston, MA 02115, USA
[e] Structural Genomics Consortium, University of Toronto, Toronto, Ontario, Canada M5G 1L5
[f] Department of Pharmacology, University of Toronto, Toronto, Ontario, Canada M5S 1A8
[g] Division of Signal Transduction, Beth Israel Deaconess Medical Center, Boston, MA 02115, USA

ARTICLE INFO

ABSTRACT

Cancer cells have distinct metabolic needs that are different from normal cells and can be exploited for development of anti-cancer therapeutics. Activation of the tumor specific M2 form of pyruvate kinase (PKM2) is a potential strategy for returning cancer cells to a metabolic state characteristic of normal cells. Here, we describe activators of PKM2 based upon a substituted thieno[3,2-b]pyrrole[3,2-d]pyridazinone scaffold. The synthesis of these agents, structure–activity relationships, analysis of activity at related targets (PKM1, PKR and PKL) and examination of aqueous solubility are investigated. These agents represent the second reported chemotype for activation of PKM2.

Published by Elsevier Ltd.

One of the most prominent distinctions between healthy and cancerous tissues is the differing energetic and nutritional needs associated with the rapid proliferative nature of cancer cells.[1,2] The original observation that cancer cells maintain a different metabolic state relative to non-proliferating cells was made by Otto Warburg in the 1920's and today the Warburg effect is a highly studied area of research.[3,4] In normal cells, glucose is primarily metabolized by glycolysis and oxidative phosphorylation when oxygen is available. Glycolysis is a multistep process that ultimately converts glucose into two equivalents of pyruvate. Further metabolism by oxidative phosphorylation involves the conversion of pyruvate to acetyl-CoA and entry into the Krebs cycle with the potential of generating additional ATP. In cancer cells this process is altered and much of the pyruvate derived from glucose is instead converted to lactic acid even in aerobic conditions. The mecha-

nism(s) that drive this altered metabolism in cancer cells are not fully understood. One contributor, however, is the differential expression of two isozymes of pyruvate kinase (PK).[5] Tanaka and coworkers were the first to show that alternative RNA splicing yields the M1 and M2 forms of pyruvate kinase (PKM1 and PKM2).[6–8] PKM2 is widely expressed in undifferentiated embryonic tissues and during development many differentiated tissues switch to express PKM1.[8–10] A second gene produces two additional PK isozymes based on alternative splicing events to produce PKL and PKR which are expressed in specific adult tissues.[11] An important realization in cancer biology was the recognition that all cancer cells express the PKM2 isozyme.[5,10,12–15]

The expression of PKM2 in cancer cells has been described as a clinical marker of malignancy for some time.[16] Pyruvate kinase catalyzes the transformation of phosphoenolpyruvate (PEP) and ADP to pyruvate and ATP when the enzyme exists as a homotetramer (dimer of dimers). Three PK isozymes (PKM2, PKL and PKR) require the binding of fructose-1,6-bis-phosphate (FBP) at an allosteric site in the tetrameric complex for activity.[17] In contrast, PKM1 does not require allosteric activation by FBP binding and retains a high affinity for PEP and high catalytic rate in its native state. Importantly, in

---

3388

J. Jiang et al. / Bioorg. Med. Chem. Lett. 20 (2010) 3387–3393

cancer cells PKM2 exists as a less active dimer with little affinity for PEP and a low catalytic rate.[5] It is theorized that down-regulation of the final step of glycolysis is a functional reason for the expression of PKM2 in cancer cells. Many glycolytic intermediates are starting points for amino acid, nucleic acid and lipid biosynthesis. Decreased pyruvate kinase activity is hypothesized to facilitate the shunting of glycolytic intermediates into these anabolic pathways required for cell growth. Hence, the expression of the less active PKM2 isozyme in cancer cells may enable anabolic processes necessary for cancer cell proliferation.
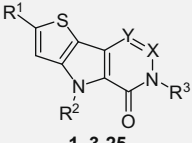
PKM1 expressing cells have a diminished capacity for tumor development in vivo relative to PKM2 expressing cells.[18] One unique property that appears to give PKM2 expressing cells this proliferative advantage is that PKM2 is a phosphotyrosine binding protein.[19] In cancer cells there is a general up-regulation of signalling events through the actions of protein kinases resulting in an elevated state of phosphorylated proteins relative to normal differentiated cells. It has been demonstrated that the binding of phosphorylated peptides to PKM2 is accompanied by the release of FBP and the further down-regulation of this enzyme. This down-regulation exacerbates the shift away from the catalytic levels associated with PKM1 and toward an anabolic state providing the needed resources for rapid proliferation.

The expression of PKM2 in cancer cells provides an attractive target for cancer therapy. Further, the observed down-regulation of PKM2 activity in cancer cells relative to the high PKM1 activity present in many normal cells suggests a therapeutic strategy whereby activation of PKM2 may restore normal cellular metabolism and, consequently, decreased cellular proliferation. To allow us to examine this possibility we have developed small molecule activators of PKM2 based upon a bis-sulfonamide scaffold previously reported[20] and the substituted thieno[3,2-*b*]pyrrole[3,2-*d*]pyridazinones reported herein.

The development of the luminescent assay detection system for pyruvate kinases and screening details were previously presented.[20–22] Akin to our earlier report, to assess the activity of the compounds described here we utilized orthogonal assays that respond to ATP or pyruvate generation by PKM2 through measurement of either firefly luciferase activity or lactate dehydrogenase (LDH) activity, respectively. The data reported in Tables 1–3 was generated in the firefly luciferase assay system.[23] A quantitative high-throughput screen (qHTS)[24] of nearly 300,000 small molecules of the NIH Molecular Libraries Small Molecule Repository was performed utilizing the firefly luciferase assay system. Numerous small molecule activators of PKM2 were identified. We ultimately selected two chemotypes for advanced interrogation. These agents are represented by the substituted thieno[3,2-*b*]pyrrole[3,2-*d*]pyridazinone **1** and substituted *N,N'*-diarylsulfonamide **2** shown in Figure 1.

In a similar manner as the recent report detailing NCGC-00030335 (**2**)[20], it was essential to establish the cooperative nature of these agents with the native substrates of PKM2. Given the allosteric activation of PKM2 by FBP, it was desirable to examine how our lead chemotypes affected the steady-state kinetics of PEP and ADP. In the absence of activator, hPK shows low affinity for PEP (K_M ~1.5 mM). In the presence of NCGC00031955 (**1**) or FBP, the K_M for PEP decreased 10-fold to 0.13 ± 0.04 mM or 0.1 ± 0.02 mM, respectively with lesser effects on V_{max} (values of 245 pmols/min with or without FBP and 255 pmols/min with or without NCGC00031955). In contrast, variation of the concentration of ADP in the presence and absence of activators shows that the steady-state kinetics are not significantly affected (K_M for ADP = 0.1 mM in either condition). Thus, NCGC00031955 (**1**) activates PKM2 by increasing the enzyme's affinity for PEP and has little effect on ADP steady-state parameters (Fig. 2A). This is similar to what we observed for FBP (Fig. 2B) which agrees with previous reports
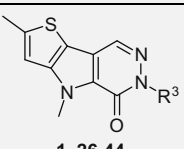
Table 1
SAR of selected thieno[3,2-*b*]pyrrole[3,2-*d*]pyridazinones and thieno[3,2-*b*]pyrrole[3,2-*d*]pyrimidinones

#	R^1	R^2	R^3	X	Y	hPK, M2 AC_{50}[a] (μM)	hPK, M2 Max. Res.[b]
1	Me	Me	2-Fluorobenzyl	N	CH	0.063	122
3	Et	Me	2-Fluorobenzyl	N	CH	0.100	105
4	*i*Pr	Me	2-Fluorobenzyl	N	CH	0.142	106
5	H	Me	2-Fluorobenzyl	N	CH	0.605	93
6	OMe	Me	2-Fluorobenzyl	N	CH	0.086	107
7	SMe	Me	2-Fluorobenzyl	N	CH	0.024	96
8	S(O)Me	Me	2-Fluorobenzyl	N	CH	0.025	98
9	S(O)$_2$Me	Me	2-Fluorobenzyl	N	CH	Inactive	NA
10	NO$_2$	Me	2-Fluorobenzyl	N	CH	0.018	113
11	NHAc	Me	2-Fluorobenzyl	N	CH	>25	59
12	CN	Me	2-Fluorobenzyl	N	CH	0.047	84
13	COOMe	Me	2-Fluorobenzyl	N	CH	0.084	70
14	CHO	Me	2-Fluorobenzyl	N	CH	0.016	100
15	CH$_2$OH	Me	2-Fluorobenzyl	N	CH	0.048	103
16	B(OH)$_2$	Me	2-Fluorobenzyl	N	CH	>10	101
17	COMe	Me	2-Fluorobenzyl	N	CH	0.011	108
18	CHOH(Me)	Me	2-Fluorobenzyl	N	CH	0.136	120
19	Me	H	2-Fluorobenzyl	N	CH	Inactive	NA
20	Me	Et	2-Fluorobenzyl	N	CH	5.9	96
21	Me	*i*Pr	2-Fluorobenzyl	N	CH	Inactive	NA
22	Me	Me	2-Fluorobenzyl	N	C(Me)	>30	56
23	H	Me	2-Fluorobenzyl	CH	N	>35	61
24	Me	Me	Phenyl	N	CH	Inactive	NA
25	Me	Me	*n*-Pentyl	N	CH	>35	47

[a] AC_{50} values were determined utilizing the luminescent pyruvate kinase-luciferase coupled assay (Ref. 21).
[b] Max. Res. value represents the % activation at 57 μM of compound. Each value is the mean from three replicate experiments.

Table 2
SAR scan of benzylated thieno[3,2-b]pyrrole[3,2-d]pyridazinones

	#	R³	hPK, M2 AC₅₀ᵃ (μM)	hPK, M2 Max. Res.ᵇ
1, 26-44	1	2-Fluorobenzyl	0.063	122
	26	Benzyl	0.062	101
	27	3-Fluorobenzyl	0.225	92
	28	4-Fluorobenzyl	0.057	102
	29	2-Chlorobenzyl	0.298	96
	30	3-Chlorobenzyl	0.126	99
	31	4-Chlorobenzyl	0.326	91
	32	4-Methylbenzyl	0.356	84
	33	4-Trifluoromethylbenzyl	0.553	56
	34	4-Methoxybenzyl	0.037	96
	35	2,4-Difluorobenzyl	0.044	96
	36	2,6-Difluorobenzyl	0.049	94
	37	2,3-Difluorobenzyl	0.215	73
	38	2-Chloro-6-fluorobenzyl	0.060	93
	39	2,3,4-Trifluorobenzyl	0.174	69
	40	2,3,5,6-Tetrafluorobenzyl	0.345	59
	41	2-Fluoro-3-methylbenzyl	0.035	97
	42	2-Fluoro-4-methylbenzyl	0.108	81
	43	2-Fluoro-4-trifluoromethylbenzyl	>15	59
	44	3-Fluoro-4-methoxybenzyl	0.225	68

ᵃ AC₅₀ values were determined utilizing the luminescent pyruvate kinase-luciferase coupled assay (Ref. 21).
ᵇ Max. Res. value represents the % activation at 57 μM of compound. Each value is the mean from three replicate experiments.

demonstrating increased affinity for PEP as the reason for activation of PKM2 by FBP.[17]

The sequence required for the chemical synthesis of NCGC00031955 (**1**) was an assembly of literature procedures (Scheme 1). Several commercially available thiophene-2-carbaldehydes were reacted with ethyl 2-azidoacetate in sodium ethoxide at 0 °C to provide the corresponding 2-azido-3-(thiophen-2-yl)acrylates. Refluxing this intermediate in o-xylene provided the core thienopyrroles in good yields.[25] Several techniques proved
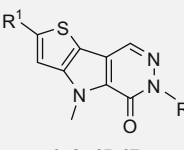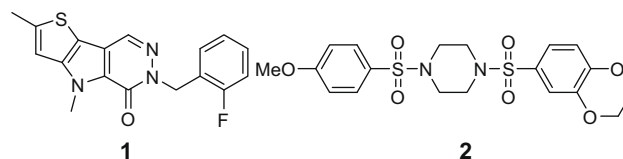

Figure 1. Chemical structures of the two lead activators of PKM2 substituted thieno[3,2-b]pyrrole[3,2-d]pyridazinone NCGC00031955 (**1**) and substituted N,N′-diarylsulfonamide NCGC00030335 (**2**).

capable of installing the needed aldehyde functionality, but ultimately we relied upon a Vilsmeier–Haack reaction to form the substituted ethyl 6-formyl-4H-thieno[3,2-b]pyrrole-5-carboxylates.[26] There was no indication of alternate regiochemical formyl installation. Through a series of experiments, we found that it was necessary to alkylate the pyrrole nitrogen before proceeding with the synthesis. This was accomplished via treatment with alkyl iodides in basic DMF. The remainder of the synthesis involved the formation of the pyridazinone via treatment with hydrazine in refluxing 2-ethoxyethanol and alkylation of the amide nitrogen with various alkyl and benzyl bromides in basic DMF.[27] Arylation of the amide nitrogen was also explored through a copper catalyzed process developed by Buchwald and co-workers.[28]

The utility of 5-bromothiophene-2-carbaldehyde as a starting reagent in this sequence (see Supplementary data) was a key to the synthetic elaboration of numerous analogues (Scheme 2). From the 2-bromo product **53** (shown in Scheme 2) we conducted numerous transformations. Treatment with sodium methoxide in refluxing 1,4-dioxane in the presence of copper iodide provided the 2-methoxy derivative **6** in good yield.[29] Copper catalysis was again used for the installation of acetamide to provide direct access to the NHAc derivative **11**.[28] The nitrile analogue **12** was achieved through treatment of the bromide with CuCN in DMF at elevated temperatures.[29] Palladium (0) catalysis, carbon monoxide and triethylamine in a MeOH/DMSO solution proved to be a successful strategy to install the methyl ester moiety of **13**. Given the lack of commercially available of 5-alkyl substituted thiophene-2-carbaldehydes we were forced to explore alternate means to examine the SAR of this position. Either vinyl or isopropenylboronic acids/pinacol esters were entered into traditional Suzuki–Miyaura couplings to provide derivatives that, upon reduction, yielded the ethyl or isopropyl derivatives **3** and **4**. Using standard reductive conditions on the starting bromide provided analogue **5** for study. Preparation of the Grignard reagent was accomplished through metal-halogen exchange and exposure of this intermediate to tri-

Table 3
SAR and solubility of selected thieno[3,2-b]pyrrole[3,2-d]pyridazinones

	#	R¹	R³	hPK, M2 AC₅₀ᵃ (μM)	hPK, M2 Max. Res.ᵇ	Solubilityᶜ (μg/mL)
1, 8, 45-47	1	Me	2-Fluorobenzyl	0.063	122	<0.2
	8	S(O)Me	2-Fluorobenzyl	0.025	98	4.4
	45	S(O)Me	3-Methoxybenzyl	0.073	99	37.4
	46	S(O)Me	3-(Methyl)aniline	0.092	93	29.6
	47	S(O)Me	3-(Methyl)phenol	0.130	102	16.9

ᵃ AC₅₀ values were determined utilizing the luminescent pyruvate kinase-luciferase coupled assay (Ref. 21) and the data represents the results from three separate experiments.
ᵇ Max. Res. value represents the % activation at 57 μM of compound.
ᶜ Kinetic solubility analysis was performed by Analiza Inc. and are based upon quantitative nitrogen detection as described (www.analiza.com). The data represents results from three separate experiments with an average intraassay %CV of 4.5%.
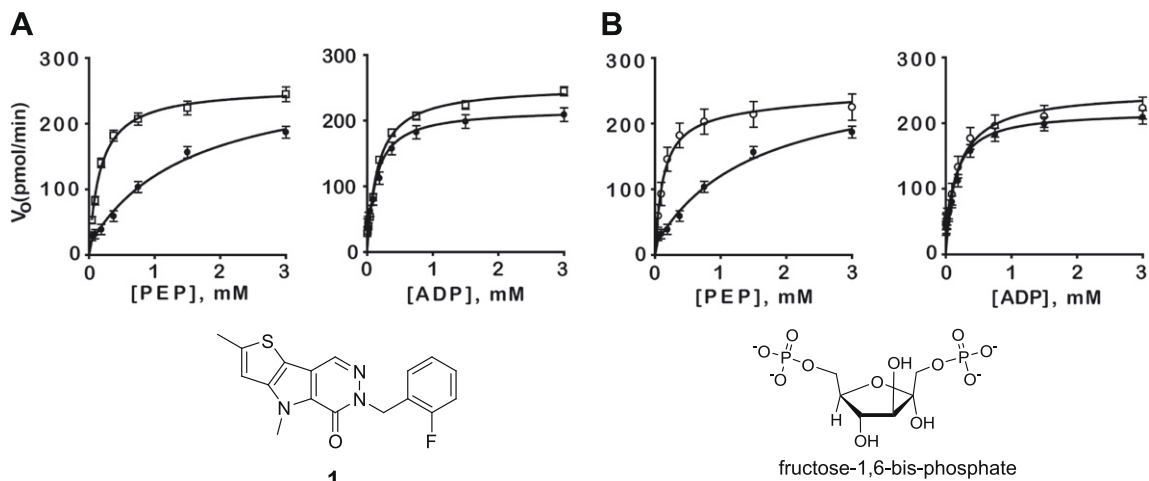
A **B**

1

fructose-1,6-bis-phosphate

Figure 2. (A) Initial velocity of PKM2 as a function of PEP and ADP concentration in the presence (open squares) or absence (filled circles) of NCGC00031955 (**1**) (10 µM). (B) Initial velocity as a function of PEP and ADP concentration in the presence (open circles) or absence (filled circles) of FBP (10 µM). V_o, initial rate in pmol/min as determined in the PK-LDH coupled assay (kinetic assays were carried out at [KCl] = 200 mM, [MgCl$_2$] = 15 mM, and with either [ADP] or [PEP] = 4.0 mM; see Supplementary data).
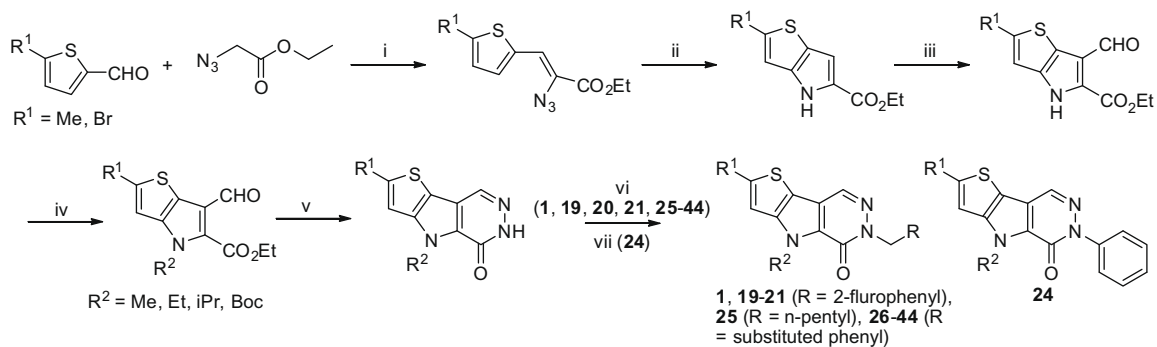
Scheme 1. Reagents and conditions: (i) Na, EtOH, 0 °C; (ii) *o*-xylene, reflux; (iii) POCl$_3$, DMF, 60 °C; (iv) R^{2}I, K$_2$CO$_3$, DMF, rt; (v) 2-ethoxyethanol, hydrazine, reflux; (vi) benzyl bromide or alkyl bromide, KO*tert*-Bu, DMF, rt; (vii) iodobenzene, CuI, *trans*-cyclohexane-1,2-diamine, 1,4-dioxane, reflux.
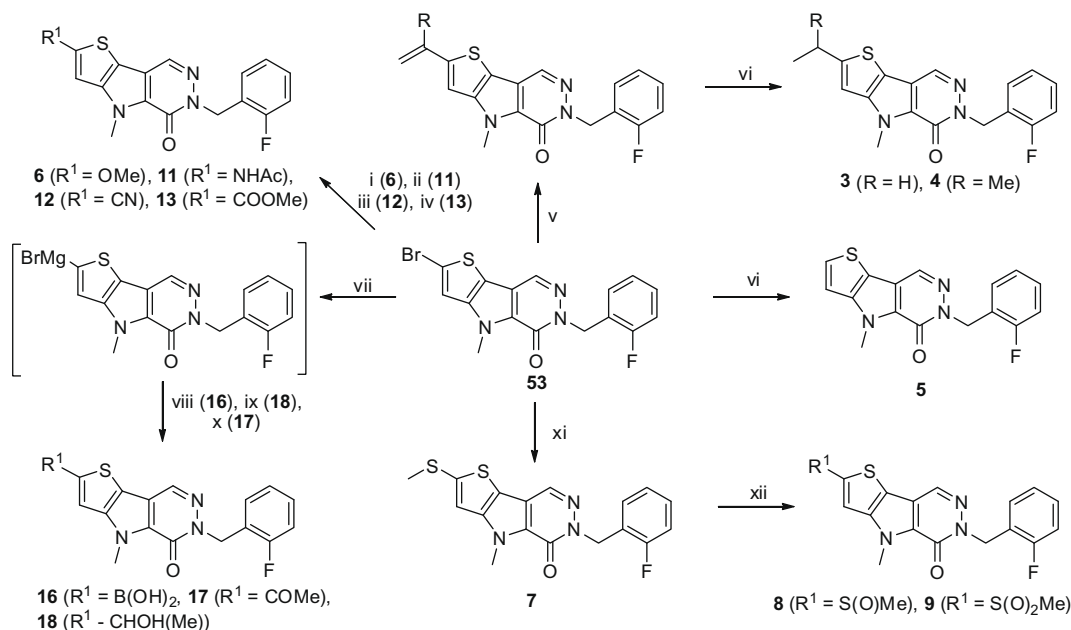
Scheme 2. Reagents and conditions: (i) Na, MeOH, CuI, 1,4-dioxane, reflux; (ii) acetamide, CuI, *trans*-cyclohexane-1,2-diamine, dioxane, reflux; (iii) CuCN, DMF, 140 °C; (iv) CO (1 atm), Pd(OAc)$_2$,1,3-bis(diphenylphosphino)propane, Et$_3$N, MeOH, DMSO, 65 °C; (v) vinyl or isopropenylboronic acid pinacol ester, Pd(PPh$_3$)$_2$Cl$_2$, 1 M Na$_2$CO$_3$/CH$_3$CN, 120 °C, microwave; (vi) Pd/C, H$_2$ (1 atm), MeOH, rt; (vii) ^{i}PrMgBr, tetramethylethylenediamine, THF, 15 °C, 20 min, then starting material, rt, 25 min; (viii) B(OMe)$_3$, 0 °C, then 0.1 N HCl; (ix) CH$_3$CHO, 0 °C; (x) procedure ix followed by IBX, DMSO, rt; (xi) NaSMe, CuBr, DMF, 140 °C; (xii) mCPBA (1.5 equiv), CH$_2$Cl$_2$, rt.

methyl borate at 0 °C followed by work-up in 0.1 N aqueous HCl provided the boronic acid analogue **16**.[30] Alternatively, quenching of the Grignard reagent with acetaldehyde provided the secondary alcohol **18** which was further oxidized to the ketone **17** with IBX in DMSO. Treatment of **53** with sodium methanethiolate and copper(I)bromide in DMF at 140 °C provided the thiol ether **7** and *m*CPBA oxidation yielded sulfoxide **8** and sulfone **9** which were separable through chromatographic methods.[31]

Our attempts to synthesize an analogue bearing a nitro group at the 2-position of the thiophene ring of the final product were met with several challenges. First, the 5-nitrothiophene-2-carbaldehyde starting material could not be converted to the azido-acrylate intermediate. Nitration of the ethyl 4*H*-thieno[3,2-*b*]pyrrole-5-carboxylate intermediate lead to nitration at both the 2 and 6 positions. While the mixture could be separated, the 2-position nitrated product could not further undergo Vilsmeier–Haack reaction. Ultimately, we relied upon nitration following installation of the aldehyde moiety at the 6-position, thus driving the nitration to the appropriate 2-position of the heterocycle (Scheme 3). The remainder of the synthesis followed a similar course. However, we did find that the formation of the pyridazinone ring was more facile proceeding in ethanol at room temperature.

We noted early that the solubility of these analogues would require improvement to generate appropriate compounds. Therefore, several mechanisms were explored to insert hydrogen bond donors into the core structure. One method for accomplishing this was to enter the un-substituted derivative **5** into a second Vilsmeier–Haack reaction at the 2-position of the thiophene ring to produce the aldehyde **14** (Scheme 4).[32] Reduction of this agent with sodium borohydride in methanol provided the alcohol **15** for examination.

One of our final SAR considerations involved changes directly on or to the pyridazinone ring. The 6-position of this ring system was the only position open for modification. To examine if substituents could be added at the lone un-substituted carbon, the aldehyde was converted to the methyl ketone through addition of a methyl Grignard reagent and IBX oxidation of the resulting secondary alcohol (Scheme 5). From this intermediate, steps iv through vi of Scheme 1 were used to produce the 6-methyl-pyridazinone version of our lead compound. A second consideration was changing from a pyridazinone to a pyrimidinone ring system (Scheme 6). To accomplish this, we took advantage of our previous observation that nitration of the ethyl 4*H*-thieno[3,2-*b*]pyrrole-5-carboxylate intermediate occurred on the 6-position of the pyrrole ring. Reduction of the nitro group was achieved via treatment with tin(II) chloride in acidic EtOH/H$_2$O and the pyrimidinone ring was formed upon condensation with ammonia formate and formamide at elevated temperatures.[33,34] The benzylation of the amide nitrogen occurred under similar conditions as previously described.

As a standard practice, NCGC00031955 (**1**) was re-synthesized and found to possess an AC$_{50}$ value of 63 nM and maximum response of 122% in the ATP generation assay system and also showed good potency and efficacy in the LDH coupled reaction (AC$_{50}$ value of 326 nM, maximum response of 224%). Our first SAR evaluations involved changes directly to the heterocyclic core structure while retaining the standard 2-fluorobenzyl substitution from the pyridazinone ring amide (Table 1). Steric expansions of the methyl group at the 2-position of the thiophene ring were typically well tolerated [for instance the ethyl and isopropyl analogues **3** (AC$_{50}$ = 100 nM, maximum response = 105%) and **4** (AC$_{50}$ = 142 nM, maximum response = 106%)]. In general, comparable potencies for these compounds were observed in
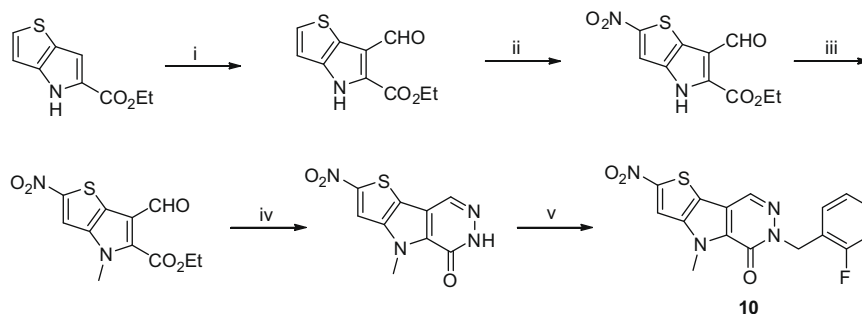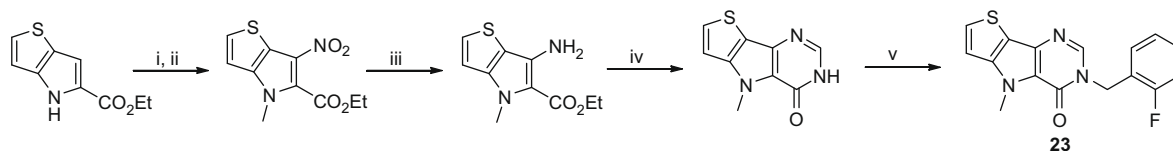

Scheme 3. Reagents and conditions: (i) POCl$_3$, DMF, 60 °C; (ii) Cu(NO$_3$)$_2$, Ac$_2$O, 0 °C to rt; (iii) MeI, K$_2$CO$_3$, DMF; (iv) hydrazine, EtOH, rt; (v) 2-fluorobenzyl bromide, K$_2$CO$_3$, DMF, rt.
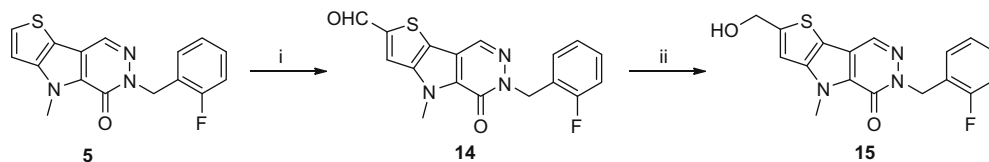
Scheme 4. Reagents: (i) POCl$_3$, DMF, ClCH$_2$CH$_2$Cl, reflux; (ii) NaBH$_4$, MeOH.
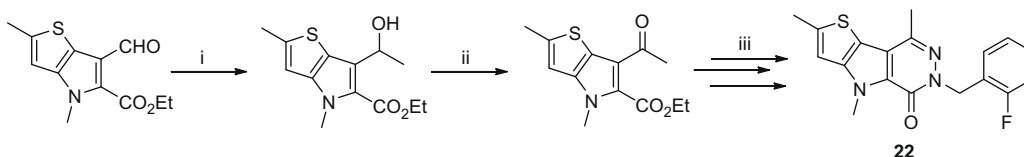
Scheme 5. Reagents and conditions: (i) MeMgCl, THF, −78 °C; (ii) IBX, DMSO, rt; (iii) steps iv through vi (Scheme 1).

Scheme 6. Reagents and conditions: (i) Cu(NO$_3$)$_2$, Ac$_2$O, 0 °C to rt; (ii) MeI, K$_2$CO$_3$, DMF; (iii) SnCl$_2$, HCl, EtOH/H$_2$O, 35 °C; (iv) NH$_2$CHO, ammonium formate, 120 °C; (v) 2-fluorobenzyl bromide, K$_2$CO$_3$, EtOH, reflux.

the LDH assay, yet the efficacies were typically 2–3-fold higher (this was a general trend for all analogues). Removal of the methyl group resulted in a loss of potency and efficacy [see **5** (AC$_{50}$ = 605 nM, maximum response = 93%)]. Insertions of heteroatoms (including oxygen and sulfur) typically resulted in improved potency including SMe [see **7** (AC$_{50}$ = 24 nM, maximum response = 96%)] and S(O)Me [see **8** (AC$_{50}$ = 25 nM, maximum response = 98%)]. Interestingly, oxidation past the sulfoxide to the sulfone resulted in a completely inactive analogue. Carbonyls and alcohols were examined and found to retain good potencies and maximum responses [for instance **14** (AC$_{50}$ = 16 nM, maximum response = 100%), **15** (AC$_{50}$ = 48 nM, maximum response = 103%) and **17** (AC$_{50}$ = 11 nM, maximum response = 108%)]. In stark contrast to substitutions on the 2-position of the thiophene ring, the methyl group on the pyrrole ring nitrogen was found to be an absolute necessity. Alterations from the methyl to the ethyl and isopropyl groups were ineffective and lack of substitution resulted in an inactive analogue as well. Further, amides and sulfonamides were examined and were not tolerated (data not shown). Addition of a methyl group to the 6 position of the pyridazinone ring was also not allowed [see **22** (AC$_{50}$ >30 μM, maximum response <80%)]. Alteration from the pyridazinone to a pyrimidinone ring system was additionally problematic [see **23** (AC$_{50}$ >35 μM, maximum response <80%)]. The necessity of the benzyl substituent was proven through examination of the corresponding phenyl analogue **24** and the *n*-pentyl analogue **25**, both of which had marked loss of potency.

Following the examination of the core heterocycle and selected appendages, a phenyl ring scan on the benzyl substituent was performed. The results suggest a less focused SAR for this moiety; however, selected trends did exist. For instance, bulky substituents were typically not successful at the *para* position of the ring [for instance **31** (AC$_{50}$ = 326 nM, maximum response = 91%), **33** (AC$_{50}$ = 553 nM, maximum response <80%) and **43** (AC$_{50}$ >15 μM, maximum response <80%)]. Electron withdrawing substitutions were typically favored [for instance **35** (AC$_{50}$ = 44 nM, maximum response = 96%), **36** (AC$_{50}$ = 49 nM, maximum response = 94%)], however examples such as the 4-methoxybenzyl analogue **34** were exceptions (AC$_{50}$ = 37 nM, maximum response = 96%).

With a better idea of the SAR for this chemotype, we next considered the aqueous solubility of these agents. Several of the most potent analogues were profiled by a commercial provider[35] of solubility and it was determined that nearly all compounds examined had aqueous solubility levels (measured in both μg/mL and μM) below detectable limits. One of the few exceptions was the sulfoxide analogue **8** which had an aqueous solubility of 4.4 μg/mL. To expand upon this result, we synthesized numerous phenyl ring analogues that maintained the key sulfoxide moiety. We choose to expand our phenyl ring scan to include aniline and phenol derivatives in hopes of gaining additional solubility. Similarly to our previous studies with the bis-sulfonamide chemotype, there was a preference for *meta*-substituted analogues (Table 3). Additionally, several of these agents possessed improved aqueous solubility including **45** (AC$_{50}$ = 73 nM, maximum response = 99%, aqueous solubility = 37.4 μg/mL), **46** (AC$_{50}$ = 92 nM, maximum response = 93%,

aqueous solubility = 29.6 μg/mL) and **47** (AC$_{50}$ = 130 nM, maximum response = 102%, aqueous solubility = 16.9 μg/mL).

With the SAR and solubility assessments established, it was essential to consider the selectivity of these compounds versus PKM1, PKR and PKL. The *N,N′*-diarylsulfonamide chemotype presented in our previous manuscript possessed a high degree of selectivity for activation of PKM2. Gratifyingly, the substituted thieno[3,2-*b*]pyrrole[3,2-*d*]pyridazinones presented here were equally selective for PKM2 activation versus PKM1. Further, all analogues examined were inactive versus PKL and PKR (see PubChem AIDs 1541, 1542, 1543, 1780, 1781, and 1782). Figure 3 details the selectivity of NCGC00031955 (**1**) versus PKM2, PKM1, PKR and PKL.

Warburg's finding that cancer cells show altered cellular respiration and metabolism ranks as one of the earliest observations in cancer biology. A key realization associated with the Warburg effect is the re-expression of PKM2 in all cancer cells leading to increased availability of glycolytic intermediates for biosynthesis of the amino acid, nucleic acid and lipid building blocks of cellular construction. The native, down-regulated kinetics of PKM2 in combination with the allosteric control of PKM2 activity by FBP and binding to phosphotyrosine proteins is an important aspect of the altered metabolic state of cancer cells. Activation of PKM2 to levels comparable to PKM1 represents an intriguing potential strategy to halt the proliferative state of cancer cells by shuttling the required glycolytic intermediates/cellular building blocks away from an anabolic state of metabolism. Here we describe a novel chemotype based upon substituted thieno[3,2-*b*]pyrrole[3,2-*d*]pyridazinone scaffold for the activation of PKM2. This agent was expanded upon via chemical synthesis and numerous SAR aspects were explored. These agents were found to increase the affinity of PKM2 for phosphoenolpyruvate (PEP) and were capable of activation responses beyond that achieved by the native allosteric activator FBP. Several agents were found with potencies below 100 nM and maximum responses ⩾FBP-mediated activation and appropriate aqueous solubility including **45**, **46** and **47**. Explorations of these agents selectivity revealed that the thieno[3,2-*b*]pyrrole[3,2-*d*]pyridazinone chemotype was selective for PKM2 with little or no activity versus PKM1, PKL and PKR. These novel activators of PKM2 provide the necessary tool compounds to explore the hypothesis that PKM2 activation will ameliorate the Warburg effect, and thereby decrease cancer cell proliferation.
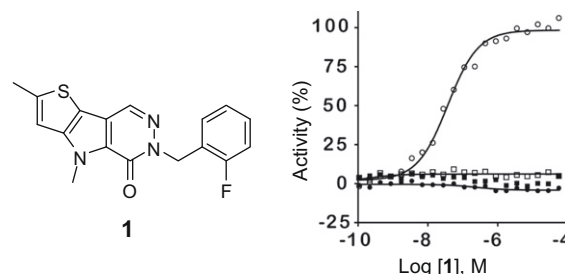

Figure 3. Selectivity assessment for NCGC00031955 (**1**) versus PKM2 (open circles), PKM1 (filled squares), PKL (open squares), and PKR (filled circles).

Acknowledgments

Supplementary data

Supplementary data (assay protocols and experimental procedures and spectroscopic data ^1H NMR, LC/MS and HRMS) associated with this article can be found, in the online version, at doi:10.1016/j.bmcl.2010.04.015.

References and notes

1. Devita, V. T., Jr.; Hellman, S.; Rosenberg, S. A. *Cancer Principles & Practice of Oncology*, 7th ed.; Lippincott Williams & Wilkins: Philadelphia (PA), 2005.
2. Vander Heiden, M. G.; Cantley, L. C.; Thompson, C. B. *Science* **2009**, *324*, 1029.
3. Warburg, O. *Science* **1956**, *123*, 309.
4. Warburg, O. *Science* **1956**, *124*, 269.
5. Mazurek, S.; Boschek, C. B.; Hugo, F.; Eigenbrodt, E. *Semin. Cancer Biol.* **2005**, *15*, 300.
6. Takenaka, M.; Noguchi, T.; Sadahiro, S.; Hirai, H.; Yamada, K.; Matsuda, T.; Imai, E.; Tanaka, T. *Eur. J. Biochem.* **1991**, *198*, 101.
7. Takenaka, M.; Yamada, K.; Lu, T.; Kang, R.; Tanaka, T.; Noguchi, T. *Eur. J. Biochem.* **1996**, *235*, 366.
8. Noguchi, T.; Inoue, H.; Tanaka, T. *J. Biol. Chem.* **1986**, *261*, 13807.
9. Yamada, K.; Noguchi, T. *Biochem. Biophys. Res. Commun.* **1999**, *256*, 257.
10. Reinacher, M.; Eigenbrodt, E. *Virchows Arch. B. Cell Pathol. Incl. Mol. Pathol.* **1981**, *37*, 79.
11. Noguchi, T.; Yamada, K.; Inoue, H.; Matsuda, T.; Tanaka, T. *J. Biol. Chem.* **1987**, *262*, 14366.
12. Staal, G. E. J.; Rijksen, G. In *Biochemical and Molecular Aspects of Selected Cancers*; Pretlow, T. G., Pretlow, T. P., Eds.; Academic Press: San Diego, 1991; p 313.
13. Steinberg, P.; Klingelhöffer, A.; Schäfer, A.; Wüst, G.; Weisse, G.; Oesch, F.; Eigenbrodt, E. *Virchows Arch.* **1999**, *434*, 313.
14. DeBerardinis, R. J.; Lum, J. J.; Hatzivassiliou, G.; Thompson, C. B. *Cell Metab.* **2008**, *7*, 11.
15. DeBerardinis, R. J.; Sayed, N.; Ditsworth, D.; Thompson, C. B. *Curr. Opin. Genet. Dev.* **2008**, *18*, 54.
16. Eigenbrodt, E.; Basenau, D.; Holthusen, S.; Mazurek, S.; Fischer, G. *Anticancer Res.* **1997**, *17*, 3153.
17. Dombrauckas, J. D.; Santarsiero, B. D.; Mesecar, A. D. *Biochemistry* **2005**, *44*, 9417.
18. Christofk, H. R.; Vander Heiden, M. G.; Harris, M. H.; Ramanathan, A.; Gerszten, R. E.; Wei, R.; Fleming, M. D.; Schreiber, S. L.; Cantley, L. C. *Nature* **2008**, *452*, 230.
19. Christofk, H. R.; Vander Heiden, M. G.; Wu, N.; Asara, J. M.; Cantley, L. C. *Nature* **2008**, *452*, 181.
20. Boxer, M. B.; Jiang, J.-K.; Vander Heiden, M. G.; Shen, M.; Skoumbourdis, A. P.; Southall, N.; Veith, H.; Leister, W.; Austin, C. P.; Park, H. W.; Inglese, J.; Cantley, L. C.; Auld, D. S.; Thomas, C. J. *J. Med. Chem.* **2010**, *53*, 1048.
21. Fan, F.; Wood, K. V. *Assay Drug Dev. Technol.* **2007**, *5*, 127.
22. Singh, P.; Harden, B. J.; Lillywhite, B. J.; Broad, P. M. *Assay Drug Dev. Technol.* **2004**, *2*, 161.
23. *Luminescent pyruvate kinase-luciferase coupled assay*. Production of a luminescent signal based on the generation of ATP by pyruvate kinase was determined by using the ATP-dependent enzyme firefly luciferase.[22] Details for the development of this assay format are provided in Ref. 20. The primary qHTS data and confirmatory data are available in PubChem (AIDs: 1631, 1634, and 1751). Follow-up of synthesized analogs was determined using the same protocol except that for the isoforms PK M1, L and R the enzyme concentration was 1 nM, 0.1 nM, and 0.1 nM, respectively (PubChem AIDs for M1, L and R bioluminescent assays are 1780, 1781, and 1782). *Fluorescent pyruvate kinase-lactate dehydrogenase coupled secondary assay*. All compounds were also tested in a kinetic mode by coupling the generation of pyruvate by pyruvate kinase to the depletion of NADH through lactate dehydrogenase.[36] Details for the development of this assay format are provided in Ref. 20. The data has been deposited in PubChem (AID: 1540). Follow-up of synthesized analogs was determined using the same protocol (PubChem AIDs for L, M1 and R bioluminescent assays are 1541, 1542, and 1543). This assay was also used to determine the K_M's for PEP and ADP in the presence and absence of activator. Conversion of fluorescent units to pmols of NADH was performed using a standard curve of known NADH concentrations. Data was collected on the Perkin Elmer Viewlux. Data was fit in GraphPad.
24. Inglese, J.; Auld, D. S.; Jadhav, A.; Johnson, R. L.; Simeonov, A.; Yasgar, A.; Zheng, W.; Austin, C. P. *Proc. Natl. Acad. Sci. U.S.A.* **2006**, *103*, 11473.
25. Eras, J.; Galvez, C.; Garcia, F. *J. Heterocycl. Chem.* **1984**, *21*, 215.
26. Bennasar, M.; Roca, T.; Ferrando, F. *J. Org. Chem.* **2005**, *70*, 9077.
27. Gale, W. E.; Scott, A. N.; Snyder, H. R. *J. Org. Chem.* **1964**, *29*, 2160.
28. Klapars, A.; Antilla, J. C.; Huang, X.; Buchwald, S. L. *J. Am. Chem. Soc.* **2001**, *123*, 7727.
29. Wu, X.; Cen, J.; Guo, H. *Faming Zhuanli Shenqing Gongkai Shuomingshu, CN* **2008**, 10035041.
30. Wang, X.; Sun, X.; Zhang, L.; Xu, Y.; Krishnamurthy, D.; Senanayake, C. H. *Org. Lett.* **2006**, *8*, 305.
31. dit Chabert, J. F.; Marquez, B.; Neville, L.; Joucla, L.; Broussous, S.; Bouhours, P.; David, E.; Pellet-Rostaing, S.; Marquet, B.; Moreau, N.; Lemaire, M. *Bioorg. Med. Chem.* **2007**, *15*, 4482.
32. Frère, P.; Raimundo, J.-M.; Blanchard, P.; Delaunay, J.; Richomme, P.; Sauvajol, J.-L.; Orduna, J.; Garin, J.; Roncali, J. *J. Org. Chem.* **2003**, *68*, 7254.
33. Marques, M. A.; Doss, R. M.; Urbach, A. R.; Dervan, P. B. *Helv. Chim. Acta* **2002**, *85*, 4485.
34. Pandey, A.; Volkots, D. L.; Seroogy, J. M.; Rose, J. W.; Yu, J.-C.; Lambing, J. L.; Hutchaleelaha, A.; Hollenbach, S. J.; Abe, K.; Giese, N. A.; Scarborough, R. M. *J. Med. Chem.* **2002**, *45*, 3772.
35. Aqueous solubility was assessed at a pH of 7.4 at room temperature from stock DMSO solutions. http://www.analiza.com/.
36. Hannaert, V.; Yernaux, C.; Rigden, D. J.; Fothergill-Gilmore, L. A.; Opperdoes, F. R.; Michels, P. A. *FEBS Lett.* **2002**, *514*, 255.